PAPER

Check for updates

Biofilm formation on collagen substrates modulates *Streptococcus mutans* bacterial extracellular nanovesicle production and cargo†

Camila Leiva-Sabadini,[a] Pablo Berríos,[a] Paula Saavedra,[a] Javiera Carrasco-Rojas, [b] José Vicente González-Aramundiz, [c] Mario Vera, [ad] Estefanía Tarifeño-Saldivia, [e] Christina M. A. P. Schuh *[b] and Sebastian Aguayo *[af]

Streptococcus mutans is the major microbial etiological agent of dental caries and can adhere to surfaces such as type-I collagen, which is present in dentin and periodontal tissues. Recent studies have characterized planktonic *S. mutans* bacterial extracellular vesicles (bEVs) at the nanoscale range and demonstrated environmental-induced changes due to sugar presence or pH alterations. However, to date, no studies have explored whether surface-derived changes can modulate bEV production in the context of oral biofilm formation in the elderly. Therefore, this work aimed to determine the role of biofilm formation and collagen glycation on the nanoscale morphology and proteomic composition of *S. mutans* bEVs. For this, bEVs from *S. mutans* biofilms on native and glycated collagen surfaces were isolated, characterized, and compared to bEVs from planktonic cells. Nanoparticle tracking analysis (NTA), atomic force microscopy (AFM), and electron microscopy confirmed bEV production and showed that bEVs from biofilms are smaller in size and less abundant than those from planktonic cells. Furthermore, proteome analysis revealed that *S. mutans* biofilm formation on native and glycated collagen led to the enrichment of several key virulence proteins. Also, a shift towards proteins involved in metabolic processes was found in bEVs following biofilm formation on collagen surfaces, whereas glucan metabolism proteins were overexpressed in vesicles from the planktonic state. These results demonstrate that biofilm formation, as well as the glycation of collagen associated with aging and hyperglycaemia, can modulate bEV characteristics and cargo and could play a central role in *S. mutans* virulence and the development of diseases such as dental caries and periodontal disease.

Introduction

Dental caries is a widespread and persistent chronic health issue, affecting around 2 billion people worldwide. Dysbiosis in the oral microbiome favours the overgrowth of cariogenic microorganisms such as *Streptococcus mutans*, leading to acid production and localized destruction of dental tissues.[1,2] Hence,

[a]Institute for Biological and Medical Engineering, Pontificia Universidad Católica de Chile, Santiago, Chile. E-mail: sebastian.aguayo@uc.cl

[b]Centro de Medicina Regenerativa, Facultad de Medicina, Clínica Alemana-Universidad del Desarrollo, Santiago, Chile. E-mail: cschuh@udd.cl

[c]Departamento de Farmacia, Facultad de Química y de Farmacia, Pontificia Universidad Católica de Chile, Santiago 7820436, Chile

[d]Departamento de Ingeniería de Minería, Escuela de Ingeniería, Pontificia Universidad Católica de Chile, Santiago, Chile

[e]Department of Biochemistry and Molecular Biology, Faculty of Biological Sciences, University of Concepción, Concepción, Chile

[f]School of Dentistry, Faculty of Medicine, Pontificia Universidad Católica de Chile, Santiago, Chile

† Electronic supplementary information (ESI) available. See DOI: https://doi.org/10.1039/d5na00248f

dental caries is considered a biofilm-mediated disease, which undergoes various stages: it starts with the adhesion of initial bacterial colonizers and progresses to biofilm formation with the production of extracellular polymeric substances (EPS) and attachment of secondary colonizers.[3] Therefore, in recent years, strong efforts have been made to understand how genetic and environmental factors such as diet, smoking, or aging, among others, can modulate the behaviour of oral biofilms to develop novel methods to prevent and treat the disease.

Among these factors, aging is of particular interest due to the significant and rapid growth of elderly populations worldwide. Furthermore, the aging process introduces distinct changes in the tissues of the oral cavity[4] such as alterations in the collagen matrix of dentin through spontaneous non-enzymatic processes forming advanced glycation end-products (AGEs).[5] These AGEs interact with dentinal collagen amino acids, particularly lysine and arginine, and alter the mechanobiological properties of the matrix.[6–8] In particular, exposure to methylglyoxal (MGO) has been demonstrated to alter the diameter, density, and number of collagen crosslinks.[9–12] Most importantly, glycation reactions are intensified in the presence of hyperglycaemia and oxidative

stress, which are major factors in type II diabetes, smoking, and cellular aging.[4,5]

Given the crucial role of collagen in the structure of dentin and periodontal tissues, it is unsurprising that oral streptococci express several collagen-binding proteins (CBPs) such as WapA and SpaP for *S. mutans*, and SrpA for *Streptococcus sanguinis*.[13–16] In this context, recent research suggests that age-related modifications of collagen (among other structural proteins) and glycation may contribute to early bacterial adhesion to oral tissues.[17–19] However, whether collagen glycation can alter other important virulence factors (*e.g.*, biofilm formation) in *S. mutans* has not yet been explored. In recent years, extracellular vesicles (EVs) have gained considerable interest, especially in facilitating and orchestrating cellular communication, tissue organization, and biofilm formation.[20,21] EVs are cell-derived nanostructures with a size of 30 to 200 nm, containing diverse cargo including proteins, lipids, nucleic acids, and sugars.[22–24] In the oral cavity, both pathogenic and non-pathogenic micro-organisms are known to secrete so-called bacterial EVs (bEVs).[25] Their production and release, by both planktonic and attached bacteria, are influenced by environmental factors such as the presence of certain nutrients and specific sugars, hypoxia, or pH.[26–28] However, it remains unknown whether *S. mutans* biofilm formation on collagen can alter bEV production compared to planktonic cells. Additionally, the impact of age-related changes, such as glycation, on the production and composition of nanoscale *S. mutans*-derived bEVs has not yet been explored.

Therefore, the aim of this work was to determine the role of collagen glycation on the morphology and composition of bEVs produced by *S. mutans* biofilms. We believe that understanding how biofilm formation and collagen glycation alter bEV production can shed light on their potential role in promoting dental caries in the elderly, paving the way for innovative nanomedicine-derived prevention and treatment strategies against biofilm formation in the future.[29,30]

Methodology

Bacterial strains and culture conditions

For all microbial assays, the well-characterized *S. mutans* UA 159 strain was employed. Stocks were kept at −80 °C and cultured on brain heart infusion (BHI) agar plates or in culture medium at 37 °C under aerobic conditions.

Collagen-coating and surface glycation

To obtain a collagen coating, tissue culture plates were incubated with type-I collagen (rat tail, 3 mg mL^{-1}, Gibco) at a concentration of 0.5 mg mL^{-1} at 37 °C for 60 min. Subsequently, the supernatants were removed and replaced with 1× phosphate-buffered saline (PBS) or glycated with 10 mM methylglyoxal (MGO), as previously described.[18] Collagen glycation was assessed as a function of collagen autofluorescence. For this, native and glycated surfaces were measured every 24 h for 4 days with a multimodal microplate reader (Synergy HT,

Biotek), utilizing black 96-well plates (excitation/emission: 360 nm/460 nm).

Biofilm formation and growth on glycated collagen substrates

For all biofilm experiments, native and glycated type-I collagen-coated 96-well plates were incubated for 72 h at 37 °C. Wells were thoroughly washed with 1× PBS to remove any unreacted collagen or MGO molecules, and 50.000 CFU of *S. mutans* were inoculated into each well with 100 µL BHI for 24 h. Subsequently, the presence of biofilms on the collagen substrates was confirmed using crystal violet (CV) staining. For this, following biofilm incubation under physiological conditions, supernatants were removed, and biofilms were washed with 1× PBS to remove loosely bound bacteria. Subsequently, samples were prepared for staining by air drying at room temperature for 15 min, followed by drying in a 60 °C oven for 30 min. Finally, plates were incubated with 0.1% CV for 15 min and subsequently washed with distilled water. Biofilms were eluted with 95% ethanol, and absorbance was measured at 562 nm on a plate reader (Synergy HT, Biotek). Furthermore, *S. mutans* biofilm formation on collagen surfaces was confirmed with AFM using the above-described methodology.

Scanning electron microscopy (SEM) of bEV production by planktonic and biofilm-bound *S. mutans*

Following incubation, both planktonic bacteria and resuspended biofilms were fixed for SEM imaging. For planktonic bacteria, samples were centrifuged at 13 000 rpm (mySPIN 12, Thermo Scientific, US) for 5 min, and the resulting pellet was resuspended in 4% paraformaldehyde (PFA) in an Eppendorf tube. Subsequently, the pellet was washed in PBS, and a droplet of bacteria was transferred to a poly-L-lysine (PLL) coated 12 mm cover slip. For biofilm samples, a droplet of the sample was transferred directly to PLL cover slips and dried for 40 min, after which 4% PFA was added. The samples were allowed to dry for 30 min and subsequently dehydrated in a series of 25%, 50%, 75% and 100% ethanol solutions for 10 min. Finally, coverslips were sputter-coated with a 5 nm gold layer and imaged with a FEI Quanta FEG250 SEM. Two cover slips were made for each condition.

bEV isolation from planktonic and collagen-bound *S. mutans* biofilms

For planktonic *S. mutans* bEV isolation, 10^7 CFU mL^{-1} cells were incubated in 100 mL BHI for 24 h at 37 °C. The samples were then vortexed vigorously and centrifuged at 4.000 rpm (NUWIND NU-C-200R-E, NuAire) for 20 min at 4 °C to sediment cells. The resulting supernatants were filtered using a 0.22 µm syringe filter. Subsequently, bEVs were isolated in two steps. First, the supernatant was concentrated with ultrafiltration (Amicon filtration system, Merck Millipore) at 4 000 rpm, 4 °C, for 15 min. Then, bEVs were pelleted with ultracentrifugation (125.000×*g*, at 4 °C, 2 h), using a T-890 fixed angle rotor (Thermo Fisher Scientific). The resulting bEV pellets were resuspended in 1× PBS and stored at −80 °C until further experimentation.

For biofilm-derived bEV isolation, collagen-coated 12-well plates were inoculated with 2 mL of BHI medium and *S. mutans* at a cell density of 1×10^7 CFU mL^{-1} at 37 °C for 24 h. Following incubation, supernatants were removed together with detached bacteria, and the resulting biofilms were harvested with a cell scraper and collected in a Falcon tube with PBS 1×. For isolation of biofilm-derived bEVs, the method described above for planktonic bacteria was employed.

bEV morphological and nanoscale characterization by transmission electron microscopy (TEM)

bEV morphology was observed with transmission electron microscopy (TEM). For this, 5 µl of each sample was transferred onto a copper grid (FCF400-NI) and counterstained with 2% uranyl acetate for 1 min, after which excess was removed with filter paper and dried at 60 °C for 20 min. Three grids were mounted for each condition. Vesicles were visualized with a Talos F200C G2 system at a magnification of 28 000× and analysed using the ImageJ software.

Nanoparticle tracking analysis (NTA)

Following isolation, nanoparticle tracking analysis (NTA, NS300, Malvern Analytical) was performed to quantify vesicle concentration and size. A 1 : 20 dilution of each sample in particle-free PBS was measured in triplicate with a camera level of 12–14 for 20 seconds. Particle size (mean) and concentration were automatically determined using the Nanosight software (NTA 3.4 Build 3.4.4) and extracted for statistical analysis from Nanosight Experiment Reports.

Atomic force microscopy (AFM) characterization

For all topographical characterization, an MFP 3D-SA atomic force microscope (AFM, Asylum Research, US) was employed with SCOUT 350 RAu silicon AFM cantilevers with a nominal spring constant of 42 N m^{-1} (NuNano, UK). Cantilever tuning was performed at a target amplitude of 2 V for biofilms and 1 V for bEVs and collagen coatings, with setpoint and gains adjusted in real time for each sample to allow optimal imaging. For sample preparation, bEV samples were placed onto a 0.1 mg mL^{-1} poly-lysine (PLL) coated glass cover slip and placed in a 50 × 9 mm Petri dish (Falcon). After immobilization on PLL-coated glass, all samples were rinsed with MilliQ water and then air dried with nitrogen gas to remove excess humidity. Topographic measurements were carried out in air at a scan size of 4 × 4 µm, 10 × 10 µm, and 20 × 20 µm for bEVs, collagen coatings, and biofilms on collagen, respectively. A scan rate of 0.7 Hz and image resolution of 256 pixels for bEVs and biofilms, and 512 pixels for collagen coatings, were employed. Finally, all AFM data and images were analysed using the Asylum Research proprietary software v.16.10.211.

Protein quantification and proteomic analysis of bEVs

Total protein quantification for bEVs was performed after sample sonication using a fluorimetric Qubit 4 (Thermo Fisher Scientific) assay according to the manufacturer's instructions.

Proteome analyses were conducted on three independent samples of planktonic bEVs and two independent samples derived from biofilm bEVs to elucidate compositional differences under planktonic and biofilm conditions. High-resolution liquid chromatography-tandem mass spectrometry (LC-MS/MS) was employed. Proteins were extracted, precipitated, and subsequently dissolved in 30 µL of 8 M urea and 25 mM ammonium bicarbonate. Reduction and alkylation were performed, followed by enzymatic digestion using trypsin (1 : 50 enzyme-to-protein ratio; Promega) at 37 °C for 16 h. Peptides were purified using disposable Evotip C18 columns (EVOSEP Biosystems) prior to LC-MS/MS analysis conducted on an Evosep One system coupled to a timsTOF PRO2 mass spectrometer (Bruker). Protein identification was carried out using MSFragger software (version 4.1), with the proteome from *S. mutans* UA 159 (UP000002512) retrieved from UniProt as the reference database. Label-free quantification (LFQ) was performed using FragPipe-Analyst. MaxLFQ intensities were calculated following median-centered normalization and Perseus-type imputation. A global threshold of 20% for non-missing values and 60% per condition was applied to ensure robust identification of proteins across conditions, while allowing for specific variability conditions (see ESI data† for extended methods).

Differential expression analyses were conducted using the limma package for pairwise comparisons between conditions (Col *vs.* Plk, MGO *vs.* Col, and MGO *vs.* Plk). Proteins were considered differentially expressed if they met the criteria of an adjusted *p*-value <0.1 and an absolute log 2 fold change >1. Functional enrichment analyses were performed on upregulated and downregulated protein subsets using DAVID. The selected enrichment terms included GOTERM Biological Process (levels 3–5), GOTERM Cellular Component (levels 3–5), and UniProt Keywords (Molecular Function and Ligand categories). Data handling and visualizations were performed in Python.
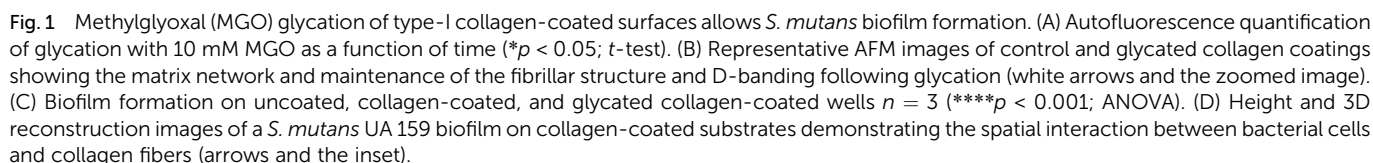
Results and discussion

Collagen-bound *S. mutans* biofilms produce EVs with specific morphological characteristics

To emulate the age-associated glycation of oral tissues *in vitro*, a previously published MGO incubation model was employed to modify collagen-coated surfaces.[11,19] AGE accumulation was monitored by collagen autofluorescence over a period of 96 h, demonstrating a significant increase in collagen glycation after exposure to MGO (Fig. 1A). The maintenance of the collagen fibrillar structure following glycation was confirmed with AFM imaging, which revealed a well-conserved collagen matrix and the presence of the characteristic nanoscale D-banding periodicity due to its molecular arrangement during fibrillogenesis (Fig. 1B). Previous work has confirmed similar observations following MGO incubation, which are in line with our present findings[11] and confirm that this glycation model is able to simulate the expected aging *in vivo* changes in fibrillar collagen.[31,32]

The ability of bacteria to use collagen as a substrate for attachment and biofilm formation in tissues is a relevant

Fig. 1 Methylglyoxal (MGO) glycation of type-I collagen-coated surfaces allows *S. mutans* biofilm formation. (A) Autofluorescence quantification of glycation with 10 mM MGO as a function of time (*$p < 0.05$; *t*-test). (B) Representative AFM images of control and glycated collagen coatings showing the matrix network and maintenance of the fibrillar structure and D-banding following glycation (white arrows and the zoomed image). (C) Biofilm formation on uncoated, collagen-coated, and glycated collagen-coated wells $n = 3$ (****$p < 0.001$; ANOVA). (D) Height and 3D reconstruction images of a *S. mutans* UA 159 biofilm on collagen-coated substrates demonstrating the spatial interaction between bacterial cells and collagen fibers (arrows and the inset).

virulence factor across many diseases and a key component of host–pathogen interactions.[16,33] In this context, biofilm formation on fibrillar collagen surfaces has been previously shown in studies with *Staphylococcus aureus* and *Porphyromonas gingivalis*, among others.[17,34] Here, we also demonstrate *S. mutans* biofilm formation on collagen-coated substrates (non-glycated and glycated), which significantly increases bacterial biomass compared to growth on uncoated well-plates (Fig. 1C). This observation is expected, considering that *S. mutans* expresses a range of CBPs – such as WapA and SpaP[16,35,36] – that have the ability to attach to collagen and facilitate the colonization of collagen-rich tissues in the human body.[16] This ability of *S. mutans* to attach to collagen is also highly relevant in the context of bacterial migration into remote tissues such as the heart and thus is associated with diseases such as endocarditis.[37,38] Furthermore, AFM imaging shows that *S. mutans* cells are intimately in contact with the collagen fibril matrix, and even are able to penetrate the superficial collagen layer (Fig. 1D, arrows). These findings are in line with previous single-cell force spectroscopy investigations, which have shown that *S. mutans* can adhere directly to collagen at the nanoscale[18] and corroborate that the biofilm is effectively anchored to the collagen surfaces and interacting with the organic matrix as expected.

bEV production by a range of clinically relevant microbes during planktonic growth has been well described;[20,39] nevertheless, there is less known regarding bEV secretion from oral biofilms. Thus, the production of bEVs by planktonic and biofilm-bound *S. mutans* cells was initially assessed using SEM (Fig. 2). Biofilm-derived cells were found to be embedded in

EPS; nevertheless, the presence of nanoscale bEVs on the surface of individualized *S. mutans* cells could be observed as previously shown[40,41] (Fig. 2B and C, arrows). Planktonic cells

Fig. 2 Ultrastructure of *S. mutans* extracellular vesicle (EV) production under biofilm and planktonic conditions. (A) Scanning electron microscopy (SEM) of adhered *S. mutans* biofilms showing extracellular polysaccharide (EPS) production and cellular aggregates. (B) and (C) High and low magnification of bEV production by biofilm-bound *S. mutans*, respectively. Low (D) and high (E) magnification of bEV production by planktonic *S. mutans*, respectively.

were also seen to produce bEVs that were visible either on the surface of cells or expanding out of the bacterial cell wall, illustrating different stages of the vesiculogenesis process[42] (Fig. 2D and E). These observations confirm that bEVs are actively produced during *S. mutans* development, spanning from its growth as a planktonic cell to its surface attachment and adoption of a biofilm lifestyle.

Following cell and biofilm growth, it was possible to isolate EVs from *S. mutans* from both collagen conditions by employing a combination of AMICON filtration and ultracentrifugation. These bacterial EVs were within the size range reported in previous literature,[20,25,43] with the largest size being found for planktonic EVs, followed by bEVs from biofilms attached to collagen and glycated collagen (124 nm, 112 nm, and 106 nm, respectively) (Fig. 3A and B). Besides the size alterations, there is a marked imaging contrast difference between bEVs from the planktonic compared to biofilm-derived vesicles, which suggests membrane composition differences among these two growth conditions. This is similar to what has previously been found in *Pseudomonas aeruginosa*, where authors found that the mode of growth (planktonic *vs.* biofilm) changed both the size and the membrane properties of bEVs.[44,45] One could speculate that biofilm-derived bEVs are smaller due to the limited resources and spatial constraints of closely packed bacteria when compared to bacteria in suspension; thus, energy would be channeled towards biofilm maintenance rather than bEV

synthesis.[46] Furthermore, planktonic bEVs were present in almost double the concentration as those isolated from biofilms; however, no differences were found regarding protein concentration across all three studied conditions (Fig. 3B). This data, paired with microscopic differences in bEV envelope composition, suggests that alterations in the cell envelope architecture may also be influencing the compositional and size characteristics of *S. mutans* bEVs that should be explored further in future studies.[47] It remains possible that the reduced yield observed for biofilm-derived vesicles is a result of bEVs being retained in the collagen matrix and not being liberated by mechanical preparation, similar to what has been recently described for matrix-bound vesicles.[48,49] Future work should seek to determine if there is persistence of *S. mutans* bEVs in the collagen matrix after biofilm removal, as it could have profound biological implications for maintaining chronic inflammation even after biofilm decontamination in the context of dental hygiene treatments.[50]

Furthermore, microscopic analysis with TEM confirmed the presence of bEVs in all the samples that were comparable to the morphology previously imaged bEVs from *S. mutans* and other microbial strains (Fig. 3A, arrows).[40,43,51] Also, AFM imaging showed that bEVs from planktonic and native collagen-bound biofilms had a higher tendency to aggregate and cluster when deposited on the surface compared to glycated collagen-derived bEVs that were found to remain more separated when
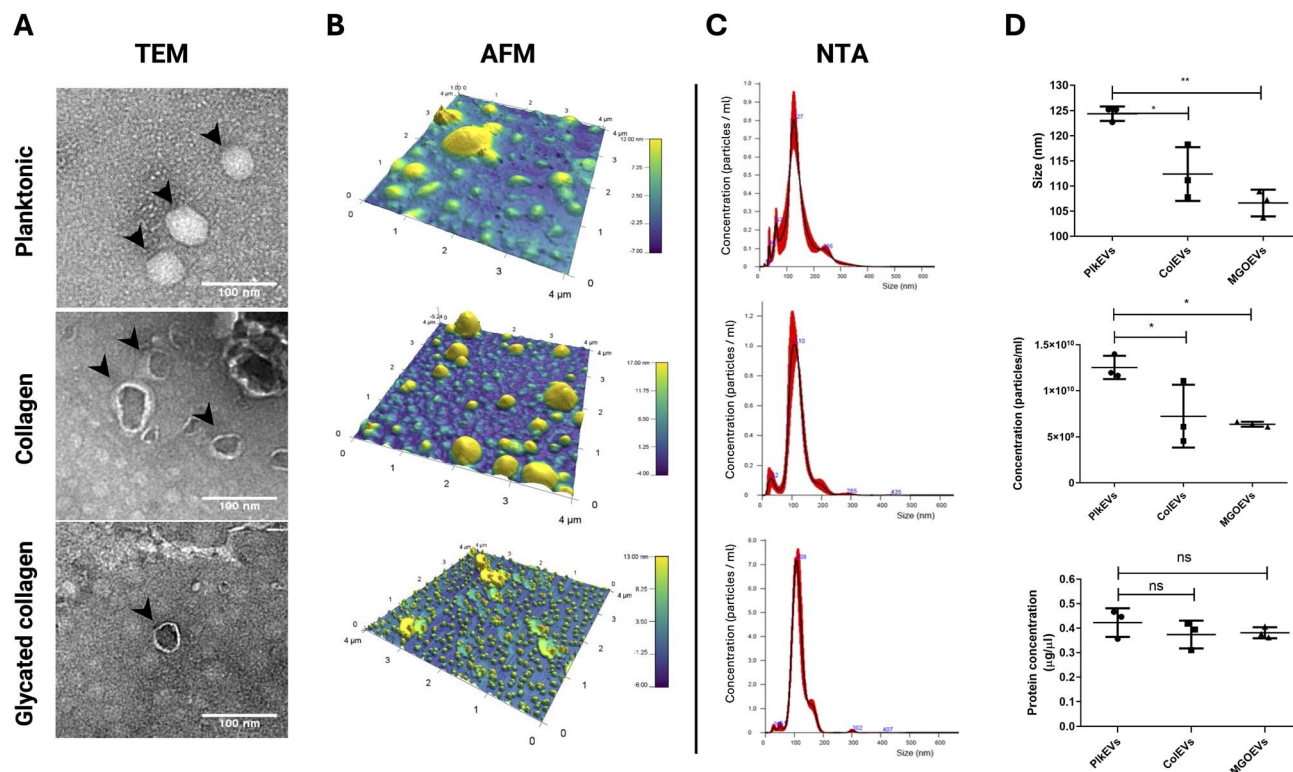

Fig. 3 Morphological and microscopic characterization of *S. mutans* UA 159 bEV production on non-glycated and glycated type-I collagen substrates. (A) Transmission electron microscopy (TEM), (B) atomic force microscopy (AFM), and (C) nanoparticle tracking analysis (NTA) for bEVs isolated from each experimental condition. (D) Size distribution, particle concentration, and protein concentration for the investigated bEVs $n = 3$ (*$p < 0.05$, **$p < 0.01$; ns: non-significant; ANOVA).

immobilized on the PLL substrates (Fig. 3A, right). This finding further suggests that growth conditions are able to induce substrate-specific changes in the surface composition of bEVs that lead to potential changes in vesicle physicochemical properties.[52]

Proteome analysis of EVs demonstrates biofilm- and glycation-induced differences in EV cargo

Subsequently, a proteome analysis of EVs isolated from all three conditions was performed. Overall, the total protein count showed 247 proteins as cargo in planktonic bEVs, 457 proteins in bEVs from collagen-bound biofilms, and 269 proteins in bEVs from glycated-collagen biofilms. Among these, 201 proteins were found to be shared across all three groups (Fig. 4A). Interestingly, bEVs across the three conditions showed the presence of the CBPs SpaP and WapA, confirming the ability of this *S. mutans* strain to form biofilms on collagen surfaces. Furthermore, the protein expression for frequently described *S. mutans* virulence factors such as GtfB, GtfC, Eno, LuxS, Tpx, and ScrB is illustrated in Fig. 4B.[53] An interesting observation is that biofilm formation on collagenous surfaces triggers an increase in protein diversity within *S. mutans* EVs when compared to bacteria in suspension (Fig. 4C, ESI data†). Furthermore, important changes in protein expression can be observed across the studied conditions and suggest that EVs from both biofilm conditions are more similar to each other than to EVs harvested from planktonic bacteria (Fig. 4C).

In contrast, the differential expression analysis revealed 237 proteins as bEV cargo that were differentially expressed in cells between planktonic and collagen, 26 between collagen and glycated collagen, and 42 between glycated collagen and planktonic (Fig. 5A, Tables 1 and 2). Thiol peroxidase (Tpx), which catalyzes the reduction of hydrogen peroxide (H_2O_2) and is involved in stress oxidative tolerance,[54] was found to be overexpressed in collagen-bound biofilm bEVs (Fig. 5B). This is clinically relevant in the context of cariogenic dysbiosis as it suggests that attachment to collagen can potentiate *S. mutans* inhibition of H_2O_2-producing commensal bacteria such as *S. sanguinis*[55] and *Streptococcus gordonii* to promote its overgrowth on the dentinal surface. This is a crucial process for the formation of *S. mutans* microcolonies that can significantly reduce the local pH and promote demineralization of the tooth surface.[56] Furthermore, overexpression in bEVs of the molecular chaperones GroES and GroEL, involved in acid stress and heat shock;[57,58] thioredoxin reductase (TrxB), part of the thioredoxin system involved in reactive oxygen species (ROS) protection;[59] glutathione reductase (GshR), that also protects cells from ROS;[60] *S*-ribosylhomocysteine (LuxS) involved in EPS synthesis, biofilm formation, and quorum sensing;[61,62] and beta-ketoacyl-[acyl-carrier-protein] synthase III (FabH) related to fatty acid synthesis in bacteria,[63] was also found in both of the collagen-
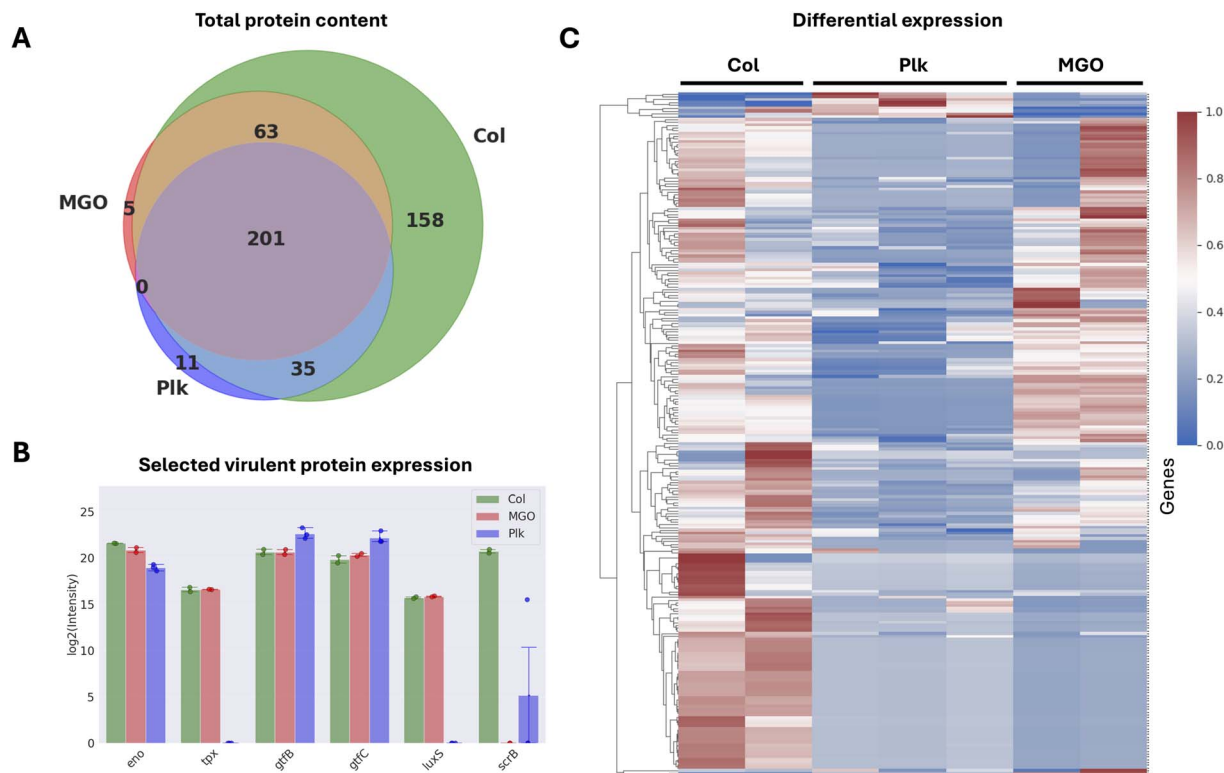

Fig. 4 Proteomics of *S. mutans* bEVs demonstrate changes following biofilm formation on collagen and surface glycation. (A) Venn diagram illustrating the total number of proteins isolated in bEVs from planktonic (Plk), collagen–bound (Col), and glycated collagen–bound (MGO) biofilms. (B) Box plot illustrating the intensity for the relevant *S. mutans* virulence proteins GtfC, ScrB, GtfB, Eno, LuxS, and Tpx across the studied bEV groups. (C) Heat map of the overall protein expression from all 3 bEV conditions (see ESI data† for extended version).
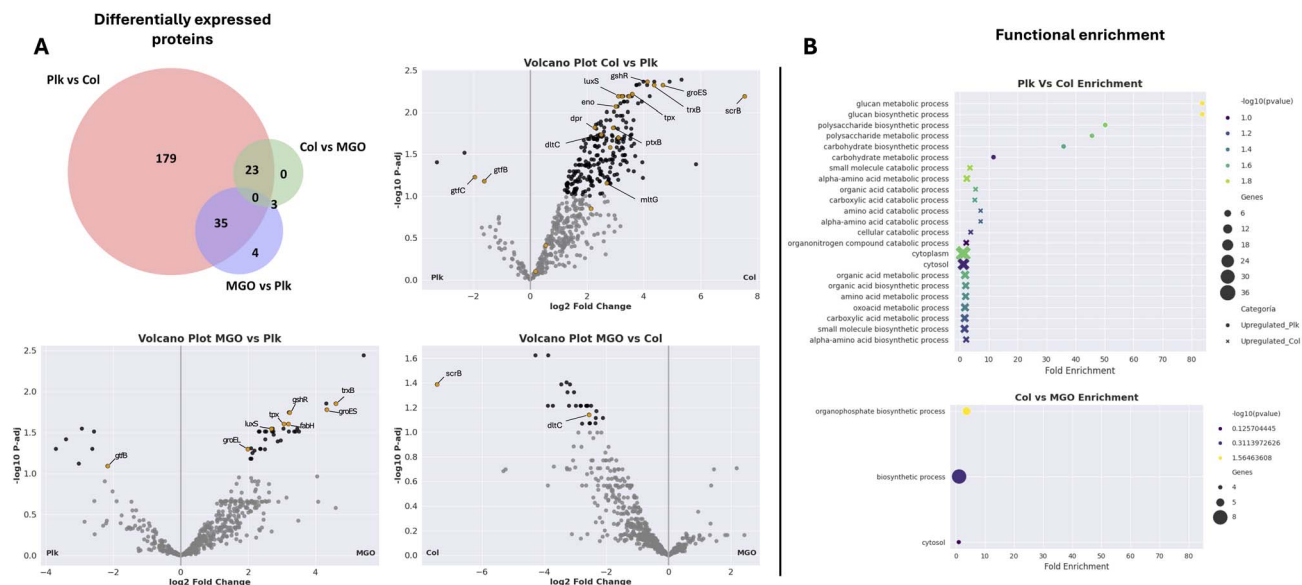
Fig. 5 Differential expression of bEV proteins as a result of biofilm formation on native and glycated collagen substrates. (A) Venn diagram of differentially expressed *S. mutans* proteins in Plk *vs.* Col, MGO *vs.* Plk, and Col *vs.* MGO bEVs. The volcano plots illustrate the upregulation of proteins in bEVs from biofilms on glycated collagen compared to the planktonic and native collagen conditions. (B) Functional enrichment maps showing the main changes in bEV protein expression following collagen attachment and collagen glycation.

Table 1 Relevant overexpressed proteins in bEVs isolated from *S. mutans* biofilm conditions (both glycated and non-glycated collagen) compared to planktonic bEVs

Protein ID	Gene	Protein description
Q8DUQ4	rpmA	Large ribosomal subunit protein bL27
Q8DWB2	pnp	Polyribonucleotide nucleotidyltransferase
Q8CWW5	groES	Co-chaperonin GroES
Q8DVL7	trxB	Thioredoxin reductase
Q8DUE5	dapA	4-Hydroxy-tetrahydrodipicolinate synthase
Q8DUR5	gshR	Glutathione reductase
P96995	galE	UDP-glucose 4-epimerase
P95787	atpA	ATP synthase subunit alpha
Q8DS44	tyrS	Tyrosine-tRNA ligase
Q8DW30	nifS	Cysteine desulfurase
Q8DUI4	thyA	Thymidylate synthase
Q8DUK3	tpx	Thiol peroxidase
Q8DTV8	ung	Uracil-DNA glycosylase
Q8DSN2	fabH	Beta-ketoacyl-[acyl-carrier-protein] synthase III
Q8DUA3	SMU_1040c	Oxidoreductase, short-chain dehydrogenase/reductase
Q8DSP7	greA	Transcription elongation factor GreA
Q8DSD8	ssb	Single-stranded DNA-binding protein
Q8DSU4	livF	Branched chain amino acid ABC transporter, ATP-binding protein
Q8DUH3	clp	Clp-like ATP-dependent protease, ATP-binding subunit
Q8DSJ5	SMU_1788c	Bacteriocin transport accessory protein, Bta
Q8CWW6	groEL	Chaperonin GroEL
Q54431	ffh	Signal recognition particle protein
Q8DVK8	luxS	S-ribosylhomocysteine lyase
Q8DS82	nusG	Transcription termination/antitermination protein NusG
Q8DTX4	SMU_1193	Transcriptional regulator
I6L8Y7	treA	Alpha,alpha-phosphotrehalase
Q8DW46	SMU_229	DhaL domain-containing protein
Q8DUE8	SMU_984	Peptidase C51 domain-containing protein
Q8DU47	SMU_1106c	Phosphoglycerate mutase
Q8DVS0	SMU_399	C3-degrading proteinase
Q9X670	pgi	Glucose-6-phosphate isomerase
Q8DTT5	SMU_1238c	Uracil-DNA glycosylase-like domain-containing protein
Q8DSX9	rplK	Large ribosomal subunit protein uL11

Table 2 Selected overexpressed virulent proteins in *S. mutans* bEVs from control collagen-bound biofilms (non-glycated) compared to bEVs from planktonic bacteria

Protein ID	Gene	Protein description
Q8DTS9	eno	Enolase
Q8DVF0	dpr	Peroxide resistance protein Dpr
I6L910	ptxB	PTS system, enzyme IIB component
Q8DVX3	YidC1	Membrane protein insertase YidC 1
Q8DSP8	YidC2	Membrane protein insertase YidC 2
Q8DSP6	mltG	Endolytic murein transglycosylase
I6L907	srtA	Sortase
Q53526	dltA	D-Alanine-D-alanyl carrier protein ligase
O70055	dltC	D-Alanyl carrier protein
Q8DUI0	clpX	ATP-dependent Clp protease ATP-binding subunit ClpX
P12655	scrA	PTS system sucrose-specific EIIBCA component

bound biofilm conditions. The vesicular overexpression of LuxS is quite relevant as it is known to be key in inter-species communication within the oral biofilm and has been shown to mediate the co-aggregation between *Porphyromonas gingivalis* and oral streptococci and induce periodontal ligament fibroblast inflammation.[64] Other biologically relevant proteins of interest that were overexpressed in bEVs isolated from biofilms include the signal recognition particle protein (Ffh) related to acid stress tolerance,[65,66] and the Clp-like ATP-dependent protease ATP-binding subunit (Clp) that is known to have a protective role in the maintenance of the bacterial proteome.[67] Therefore, it remains possible that *S. mutans* bEVs are playing a role in modifying the local ecology towards dysbiosis following its attachment to native and glycated collagen in tissues, implying a role not only in dental caries but also periodontal disease modulation.

In addition to those mentioned above, collagen-derived bEVs displayed other relevant overexpressed proteins such as enolase (Eno), a glycolytic enzyme that can translocate to the cell wall to act as a plasminogen receptor to bind human plasminogen,[68,69] and thus is believed to be involved in *S. mutans* remote tissue invasion and infective endocarditis.[70] Also, the increase of peroxide resistance protein (Dpr) involved in ROS protection;[54] the phosphor transferase system enzyme IIB component (PtxB) involved in biofilm development and acid response;[71] the ATP-dependent Clp protease ATP-binding subunit (ClpX) that modulates *S. mutans* virulence;[72,73] the sucrose-6-phosphate hydrolase (ScrB) and PTS system sucrose-specific EIIBCA component (ScrA), essential for sucrose internalization;[74] the membrane protein insertases (YidC1) and (YidC2) related to biofilm formation, protein secretion, and cell surface biogenesis;[75] and endolytic murein transglycolase (MltG) related to peripheral peptidoglycan synthesis[76] were also found in bEVs isolated from biofilms attached to native collagen surfaces. Furthermore, bEVs from this condition displayed an overexpression of sortase (SrtA), a highly relevant enzyme that enables the anchoring of collagen-binding proteins such as SpaP and WapA to the *S. mutans* cell wall, and as such, can promote *S. mutans* adhesion and subsequent biofilm formation on collagen surfaces.[16,77,78] Regarding the comparison between the non-glycated and glycated collagen biofilm groups, an overexpression of ScrB and the d-alanyl carrier protein (Dltc) associated with lipoteichoic acid metabolism[62,79] was also observed (Fig. 4C).

Biological relevance of *S. mutans* bEV modulation as a function of surface attachment and glycation

As a final step, an enrichment analysis of the *S. mutans* bEV proteome as a function of biofilm formation was carried out (Fig. 5B). It was found that proteins involved in glucan synthesis processes were enriched in bEVs obtained from planktonic conditions compared to bEVs obtained from biofilms. In addition, biofilm formation on collagen promoted the packaging of proteins involved in several metabolic pathways within bEVs. Finally, collagen glycation was found to reduce the enrichment of biosynthetic proteins inside bEVs compared to the ones obtained on native collagen surfaces (Fig. 5B). These findings suggest that when *S. mutans* bacteria are in a planktonic state – such as floating in saliva or crevicular fluid –they overexpress Gtfs in their bEVs to promote EPS formation in their surrounding environment with the goal of attaching to surfaces and forming a biofilm.[53] Once adhered, however, they switch to packaging metabolic proteins in order to kickstart biofilm formation and quorum sensing by the surrounding bacterial cells. This, in conjunction with a higher content of Tpx, can lead to a competitive advantage for *S. mutans versus* other early-colonizing commensal oral streptococci.[55] Also, as recent reports show that *S. mutans* bEVs have an inflammatory impact on host tissue cells,[80] questions remain regarding how changes in bEV composition may impact host–pathogen interactions in the context of oral inflammation that should be explored in the future.

From our current results, it seems that bacterial adhesion alone is enough to induce changes in the compositional (Fig. 2 and 3) and secretory (Fig. 4 and 5) profiles of *S. mutans* bEVs without the need for other environmental changes such as nutrient availability, flow, or pH alterations. It is well known that bacterial adhesion to surfaces and biofilm formation cause relevant changes in microbial transcription compared to planktonic cells.[81] Our present work demonstrates that these changes also hold true regarding the packaging of proteins in bEVs by *S. mutans*. To the best of our knowledge, this work is the

first to show that biofilm formation on collagen can modulate the protein content of *S. mutans* EVs and suggests that this process is an important virulence factor in the development of oral diseases.

In contrast, saliva poses a significant challenge to bacterial communication and survival due to the presence of redox-active molecules, proteases, and immune components.[82,83] In this context, proteolytic enzymes can degrade bacterial proteins involved in bacterial communication and biofilm formation, and secretory immunological molecules can rapidly neutralize the bacterial surface and secreted proteins. These environmental pressures likely drive oral bacteria to employ protective strategies such as packaging key proteins and molecules in bEVs to shield them from salivary inactivation. Therefore, it is no surprise that *S. mutans* bEVs contain many virulent proteins, including LuxS, Gtfs, and TrxB, among others, which are probably being trafficked as part of quorum sensing mechanisms among bacteria. In this context, future work should explore whether these bEVs also mediate inter-species communication and quorum sensing within polymicrobial biofilms and drive the establishment and progression of local and systemic infections. Furthermore, how these alterations in bEV cargo may act synergistically with other glycation-induced changes that directly affect bacterial cells and biofilms – such as increased adhesion and extracellular DNA secretion – remains to be elucidated.[18,84]

Conclusion

S. mutans bEV production is modulated by both collagen attachment and surface glycation by MGO. Biofilm cells were found to produce smaller bEVs as well as reduced particle yields when compared to planktonic *S. mutans*, although biofilms on glycated surfaces resulted in less bEV aggregation. Furthermore, important changes in bEV protein cargo and expression were observed as a result of biofilm formation and glycation, including crucial virulence factors such as GtfB, GtfC, Eno, LuxS, Tpx, and ScrB that are involved in key processes associated with biofilm formation. Also, a compositional shift towards the packaging of proteins involved in metabolic processes was found following biofilm formation on collagen surfaces. Overall, the present results suggest that biofilm formation on both native and glycated collagen surfaces modulates bEV production and cargo and may play an important role in *S. mutans* virulence and the development of oral disease.

Data availability

Data supporting this work can be found in this article, in the ESI data,† and posted on Figshare (**https://doi.org/10.6084/m9.figshare.29518496.v1**).

Conflicts of interest

There are no conflicts to declare.

Acknowledgements

References

1 N. B. Pitts, D. T. Zero, P. D. Marsh, K. Ekstrand, J. A. Weintraub, F. Ramos-Gomez, J. Tagami, S. Twetman, G. Tsakos and A. Ismail, *Nat. Rev. Dis. Primers*, 2017, **3**, 1–16.

2 N. J. Kassebaum, E. Bernabé, M. Dahiya, B. Bhandari, C. J. L. Murray and W. Marcenes, *J. Dent. Res.*, 2015, **94**, 650–658.

3 G. S. Khalid, M. H. Hamrah, E. S. Ghafary, S. Hosseini and F. Almasi, *Drug Des. Devel. Ther.*, 2021, **15**, 1149–1156.

4 I. B. Lamster, L. Asadourian, T. Del Carmen and P. K. Friedman, *Periodontol*, 2000, **72**, 96–107.

5 C.-S. Kim, S. Park and J. Kim, *J. Exerc. Nutrition Biochem.*, 2017, **21**, 55–61.

6 C. M. A. P. Schuh, C. Leiva-Sabadini, S. Huang, N. P. Barrera, L. Bozec and S. Aguayo, *J. Dent. Res.*, 2022, **101**, 840–847.

7 F. Greis, A. Reckert, K. Fischer and S. Ritz-Timme, *Int. J. Legal Med.*, 2018, **3**, 799–805.

8 Y. Shinno, T. Ishimoto, M. Saito, R. Uemura, M. Arino, K. Marumo, T. Nakano and M. Hayashi, *Sci. Rep.*, 2016, **6**, 19849.

9 K. Nowotny, J. P. Castro, M. Hugo, S. Braune, D. Weber, M. Pignitter, V. Somoza, J. Bornhorst, T. Schwerdtle and T. Grune, *Free Radical Biol. Med.*, 2018, **120**, 102–113.

10 K. Sugiura, S. Koike, T. Suzuki and Y. Ogasawara, *Biochem. Biophys. Res. Commun.*, 2021, **562**, 100–104.

11 M. Vaez, M. Asgari, L. Hirvonen, G. Bakir, E. Khattignavong, M. Ezzo, S. Aguayo, C. M. Schuh, K. Gough and L. Bozec, *Acta Biomater.*, 2023, **155**, 182–198.

12 S. Álvarez, J. Morales, P. Tiozzo-Lyon, P. Berrios, V. Barraza, K. Simpson, A. Ravasio, X. Monforte Vila, A. Teuschl-Woller, C. M. A. P. Schuh and S. Aguayo, *Lab Chip*, 2024, **24**, 1648–1657.

13 R. Nomura, M. Otsugu, M. Hamada, S. Matayoshi, N. Teramoto, N. Iwashita, S. Naka, M. Matsumoto-Nakano and K. Nakano, *Sci. Rep.*, 2020, **10**, 1–14.

14 A. Avilés-Reyes, J. H. Miller, J. A. Lemos and J. Abranches, *Mol. Oral Microbiol.*, 2017, **32**, 89–106.

15 C. Plummer, H. Wu, S. W. Kerrigan, G. Meade, D. Cox and C. W. I. Douglas, *Br. J. Haematol.*, 2005, **129**, 101–109.

16 S. Álvarez, C. Leiva-Sabadini, C. M. A. P. Schuh and S. Aguayo, *Crit. Rev. Microbiol.*, 2021, 1–13.

17 M. Śmiga, J. W. Smalley, P. Ślęzak, J. L. Brown, K. Siemińska, R. E. Jenkins, E. A. Yates and T. Olczak, *Int. J. Mol. Sci.*, 2021, **21**, 1–19.

18 C. Leiva-Sabadini, P. Tiozzo-Lyon, L. Hidalgo-Galleguillos, L. Rivas, A. I. Robles, A. Fierro, N. P. Barrera, L. Bozec,

C. M. A. P. Schuh and S. Aguayo, *J. Dent. Res.*, 2023, **102**, 957–964.

19 C. M. A. P. Schuh, B. Benso, P. A. Naulin, N. P. Barrera, L. Bozec and S. Aguayo, *J. Dent. Res.*, 2020, **100**, 82–89.

20 G.-J. Jeong, F. Khan, N. Tabassum, K.-J. Cho and Y.-M. Kim, *Acta Biomater.*, 2024, **178**, 13–23.

21 G. Berumen Sánchez, K. E. Bunn, H. H. Pua and M. Rafat, *Cell Commun. Signaling*, 2021, **19**, 104.

22 E. I. Buzas, *Nat. Rev. Immunol.*, 2023, **23**, 236–250.

23 L. M. Doyle and M. Z. Wang, *Cells*, 2019, **7**, 1–24.

24 N. Chen, Y. Li, X. Liang, K. Qin, Y. Zhang, J. Wang, Q. Wu, T. B. Gupta and Y. Ding, *Biofilm*, 2024, **8**, 100216.

25 C. Leiva-Sabadini, P. Saavedra, C. Inostroza and S. Aguayo, *Crit. Rev. Microbiol.*, 2024, 1–18.

26 R. Martínez-López, M. L. Hernáez, E. Redondo, G. Calvo, S. Radau, M. Pardo, C. Gil and L. Monteoliva, *Microbiol. Spectrum*, 2022, **10**, 1–21.

27 R. Wu, Y. Tao, Y. Cao, Y. Zhou and H. Lin, *Front. Microbiol.*, 2020, **11**, 1–14.

28 E. Helliwell, D. Choi, J. Merritt and J. Kreth, *ISME J.*, 2023, **17**, 1430–1444.

29 S. Malik and Y. Waheed, *Dent. J.*, 2023, **11**, 266.

30 Y. Xie, H. Liu, Z. Teng, J. Ma and G. Liu, *Nanoscale*, 2025, **17**, 5605–5628.

31 D. Sloseris and N. R. Forde, *Matrix Biol.*, 2025, **135**, 153–160.

32 E. Quansah, T. A. Shaik, E. Çevik, X. Wang, C. Höppener, T. Meyer-Zedler, V. Deckert, M. Schmitt, J. Popp and C. Krafft, *Anal. Bioanal. Chem.*, 2023, **415**, 6257–6267.

33 R. Nomura, Y. Ogaya and K. Nakano, *PLoS One*, 2016, **11**, e0159613.

34 P. Herman-Bausier, C. Valotteau, G. Pietrocola, S. Rindi, D. Alsteens, T. J. Foster, P. Speziale and Y. F. Dufrêne, *mBio*, 2016, **7**, 1–11.

35 L. Zhu, J. Kreth, S. E. Cross, J. K. Gimzewski, W. Shi and F. Qi, *Microbiol.*, 2006, **152**, 2395–2404.

36 M. Soell, J. Hemmerlé, M. Hannig, Y. Haïkel, H. Sano and D. Selimovic, *Eur. J. Oral Sci.*, 2010, **118**, 590–595.

37 T. K. Han, C. Zhang and M. L. Dao, *Biochem. Biophys. Res. Commun.*, 2006, **343**, 787–792.

38 R. Nomura, M. Otsugu, S. Naka, N. Teramoto, A. Kojima, Y. Muranaka, M. Matsumoto-Nakano, T. Ooshima and K. Nakano, *Infect. Immun.*, 2014, **82**, 5223–5234.

39 N. De Langhe, S. Van Dorpe, N. Guilbert, A. Vander Cruyssen, Q. Roux, S. Deville, S. Dedeyne, P. Tummers, H. Denys, L. Vandekerckhove, O. De Wever and A. Hendrix, *Nat. Commun.*, 2024, **15**, 9410.

40 S. Liao, M. I. Klein, K. P. Heim, Y. Fan, J. P. Bitoun, S. J. Ahn, R. A. Burne, H. Koo, L. J. Brady and Z. T. Wen, *J. Bacteriol.*, 2014, **196**, 2355–2366.

41 U. Resch, J. A. Tatsaronis, A. Le Rhun, G. Stübiger, M. Rohde, S. Kasvandik, S. Holzmeister, P. Tinnefeld, S. N. Wai and E. Charpentier, *mBio*, 2016, **7**, 1–10.

42 J. Xie, F. Haesebrouck, L. Van Hoecke and R. E. Vandenbroucke, *Trends Microbiol.*, 2023, **31**, 1206–1224.

43 Y. Cao, Y. Zhou, D. Chen, R. Wu, L. Guo and H. Lin, *Appl. Microbiol. Biotechnol.*, 2020, **104**, 9733–9748.

44 J. E. L, Z. Lauren, B. N. J, P. Steve, H. A. F and K.-L. Maria, *Microbiol. Spectrum*, 2023, **11**, e05179.

45 N. Mozaheb, P. Van Der Smissen, T. Opsomer, E. Mignolet, R. Terrasi, A. Paquot, Y. Larondelle, W. Dehaen, G. G. Muccioli and M.-P. Mingeot-Leclercq, *mSphere*, 2022, **7**, 1–13.

46 Y. Zhang, Y. Cai, B. Zhang and Y.-H. P. J. Zhang, *Nat. Commun.*, 2024, **15**, 7575.

47 V. C. Salgueiro-Toledo, J. Bertol, C. Gutierrez, J. L. Serrano-Mestre, N. Ferrer-Luzon, L. Vázquez-Iniesta, A. Palacios, L. Pasquina-Lemonche, A. Espaillat, L. Lerma, B. Weinrick, J. L. Lavin, F. Elortza, M. Azkargorta, A. Prieto, P. Buendía-Nacarino, J. L. Luque-García, O. Neyrolles, F. Cava, J. K. Hobbs, J. Sanz and R. Prados-Rosales, *Elife*, 2025, **13**, 1–38.

48 L. M. Piening and R. A. Wachs, *Cells Tissues Organs*, 2023, **212**, 111–123.

49 D. Di Francesco, C. Di Varsavia, S. Casarella, E. Donetti, M. Manfredi, D. Mantovani and F. Boccafoschi, *Int. J. Mol. Sci.*, 2024, **25**, 1–17.

50 C. M. Cobb and J. S. Sottosanti, *J. Periodontol.*, 2021, **92**, 1370–1378.

51 X. Wang, C. D. Thompson, C. Weidenmaier and J. C. Lee, *Nat. Commun.*, 2018, **9**, 1379.

52 J. Yi, S. Kim, C. Han and J. Park, *Analyst*, 2024, **149**, 5638–5648.

53 Q. Zhang, Q. Ma, Y. Wang, H. Wu and J. Zou, *Int. J. Oral Sci.*, 2021, **13**, 30.

54 T. R. Ruxin, J. A. Schwartzman, C. R. Davidowitz, Z. Peters, A. Holtz, R. A. Haney and G. A. Spatafora, *J. Bacteriol.*, 2021, **203**, 1–16.

55 R. A. Giacaman, S. Torres, Y. Gómez, C. Muñoz-Sandoval and J. Kreth, *Arch. Oral Biol.*, 2015, **60**, 154–159.

56 D. Kim, J. P. Barraza, R. A. Arthur, A. Hara, K. Lewis, Y. Liu, E. L. Scisci, E. Hajishengallis, M. Whiteley and H. Koo, *Proc. Natl. Acad. Sci. U. S. A.*, 2020, **117**, 12375–12386.

57 Z. T. Wen, P. Suntharaligham, D. G. Cvitkovitch and R. A. Burne, *Infect. Immun.*, 2005, **73**, 219–225.

58 M. Bolean, T. de P. Paulino, G. Thedei and P. Ciancaglini, *Photomed. Laser Surg.*, 2010, **28**, S79–S84.

59 S. Marco, R. Rullo, A. Albino, M. Masullo, E. De Vendittis and M. Amato, *Biochimie*, 2013, **95**, 2145–2156.

60 S. D. Pophaly, R. Singh, S. D. Pophaly, J. K. Kaushik and S. K. Tomar, *Microb. Cell Fact.*, 2012, **11**, 114.

61 J. Merritt, F. Qi, S. D. Goodman, M. H. Anderson and W. Shi, *Infect. Immun.*, 2003, **71**, 1972–1979.

62 M. I. Klein, J. Xiao, B. Lu, C. M. Delahunty, J. R. Yates and H. Koo, *PLoS One*, 2012, **7**, e45795.

63 C.-Y. Lai and J. E. Cronan, *J. Biol. Chem.*, 2003, **278**, 51494–51503.

64 N. Scheres, R. J. Lamont, W. Crielaard and B. P. Krom, *Anaerobe*, 2015, **35**, 3–9.

65 J. A. Gutierrez, P. J. Crowley, D. G. Cvitkovitch, L. J. Brady, I. R. Hamilton, J. D. Hillman and A. S. Bleiweis, *Microbiology*, 1999, **145**, 357–366.

66 P. J. Crowley, G. Svensäter, J. L. Snoep, A. S. Bleiweis and L. J. Brady, *FEMS Microbiol. Lett.*, 2006, **234**, 315–324.

67 S. D. Pandey and I. Biswas, *Microbiologyopen*, 2022, **11**, e1288.

68 M. N. Jones and R. G. Holt, *Biochem. Biophys. Res. Commun.*, 2007, **364**, 924–929.

69 J. Ge, D. M. Catt and R. L. Gregory, *Infect. Immun.*, 2004, **72**, 6748–6752.

70 S. Chamat-Hedemand, A. Dahl, L. Østergaard, M. Arpi, E. Fosbøl, J. Boel, L. B. Oestergaard, T. K. Lauridsen, G. Gislason, C. Torp-Pedersen and N. E. Bruun, *Circulation*, 2020, **142**, 720–730.

71 X. Wu, J. Hou, X. Chen, X. Chen and W. Zhao, *BMC Microbiol.*, 2016, **16**, 51.

72 J. K. Kajfasz, A. R. Martinez, I. Rivera-Ramos, J. Abranches, H. Koo, R. G. Quivey Jr and J. A. Lemos, *J. Bacteriol.*, 2009, **191**, 2060–2068.

73 G. Vivek, B. Saswati and B. Indranil, *Microbiol. Spectrum*, 2023, **12**, e03457–23.

74 Z. Lin and B. R. A, *J. Bacteriol.*, 2013, **195**, 833–843.

75 S. R. Palmer, P. J. Crowley, M. W. Oli, M. A. Ruelf, S. M. Michalek and L. J. Brady, *Microbiology*, 2012, **158**, 1702–1712.

76 S. Zaidi, K. Ali, Y. M. Chawla and A. U. Khan, *AMB Express*, 2023, **13**, 19.

77 M.-Y. Li, R.-J. Huang, X.-D. Zhou and R. L. Gregory, *Int. J. Oral Sci.*, 2013, **5**, 206–211.

78 X. Chen, C. Liu, X. Peng, Y. He, H. Liu, Y. Song, K. Xiong and L. Zou, *Mol. Oral Microbiol.*, 2019, **34**, 219–233.

79 Y. Mazda, M. Kawada-Matsuo, K. Kanbara, Y. Oogai, Y. Shibata, Y. Yamashita, S. Miyawaki and H. Komatsuzawa, *Mol. Oral Microbiol.*, 2012, **27**, 124–135.

80 G. Song, M. Li, B. Zhou, H. Qi and J. Guo, *Microb. Pathog.*, 2024, **196**, 106994.

81 M. C. Sánchez, P. Romero-Lastra, H. Ribeiro-Vidal, A. Llama-Palacios, E. Figuero, D. Herrera and M. Sanz, *BMC Microbiol.*, 2019, **19**, 58.

82 P. Brandtzaeg, *J. Oral Microbiol.*, 2013, **5**, 20401.

83 B. Čižmárová, V. Tomečková, B. Hubková, A. Hurajtová, J. Ohlasová and A. Birková, *Int. J. Mol. Sci.*, 2022, **23**, 1–21.

84 X. Xie, X. Liu, Y. Li, L. Luo, W. Yuan, B. Chen, G. Liang, R. Shen, H. Li, S. Huang and C. Duan, *Front. Microbiol.*, 2020, **11**, 1–12.